

Vorticity transport in solidification boundary layers

By BARRY L. REED¹, AMIR H. HIRSA²
AND PAUL H. STEEN^{1,3}

¹School of Chemical Engineering, Cornell University, Ithaca, NY 14853, USA

²Department of Mechanical Engineering, Aeronautical Engineering & Mechanics,
Rensselaer Polytechnic Institute, Troy, NY 12180 USA

³Center for Applied Mathematics, Cornell University Ithaca, NY 14853, USA

(Received 19 July 2000 and in revised form 6 September 2000)

A solidification boundary layer, where vorticity is concentrated, is shown to scale as $\delta \sim (v/V) \sin \theta$ where θ is the angle that the solidification front makes with the oncoming flow, v is the kinematic viscosity of the melt, and V is the solidification rate. Key similarities with the suction boundary layer are outlined. Transport of vorticity, by diffusion and advection, in flows that solidify is discussed in the context of the planar-flow spin casting process, with special attention paid to how vorticity leaves the flow. Direct experimental evidence for a solidification layer in that application is reported.

1. Introduction

The flux of vorticity ω at a solid boundary (normal direction, y) is given in a two-dimensional flow by the pressure gradient along the boundary (tangential direction, x),

$$-v d\omega/dy = \rho^{-1} dp/dx, \quad (1.1)$$

where v is the kinematic viscosity and ρ is the density of the fluid. The significance of this boundary condition has long been appreciated (e.g. Lighthill 1963). In forming operations involving a solidifying flow, a material starts in the molten state and ends as a solid, and so initially there is vorticity and finally there is none. Here we seek to better understand the vorticity budget and distribution in flows that solidify.

We shall assume incompressible Newtonian behaviour. Molten metals are indeed Newtonian if the solidification front is sharp. Density change on phase change is also neglected, for simplicity. We limit our scope to steady, nearly inviscid flows with solidification confined to a linear front and without the effects of buoyancy. This is perhaps the simplest extension of vorticity transport in classical boundary layers to include freezing. Yet it is an extension of relevance to applications. The planar-flow casting application will be described below with justification of the above simplifications. In the remainder of this introduction, we examine the essential features of the solidification boundary layer, likely to be relevant to a range of applications. The reader who would benefit from a more detailed motivation from the viewpoint of a particular application should now read the first few paragraphs of §4 and return thereafter.

Solidification boundary layers occur when solidification rates are sufficiently rapid

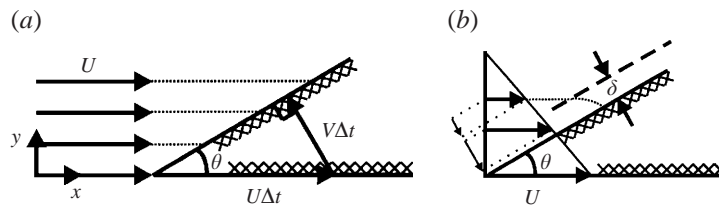


FIGURE 1. Solidifying inviscid (a) and nearly inviscid (b) flows.

to drive nearly inviscid flows. Figure 1(a) illustrates the idealized situation. Material freezes at a constant rate V against a substrate that moves at a rate U . A linear interface of phase change (solidification front) is stationary in the laboratory frame provided the freeze rate just balances the removal rate, or $V = U \sin \theta$, in which case, a wedge of 'product' of angle θ forms. The velocity triangle shown in figure 1(a) is the 'freeze' triangle, or triangle appropriate to the solid side of the front.

A velocity triangle may also be constructed on the liquid side, the 'feed' triangle, which will depend on the feed velocity. The boundary conditions on the liquid side require a component normal to the front that supplies the solidifying material and a component tangential to the front that satisfies no-slip relative to the moving solid (e.g. Glicksman, Coriell & McFadden 1986). An overall mass balance requires that the freeze rate just balance the feed rate. This is achieved without any mismatch in boundary velocities by the uniform horizontal flow of speed U shown in figure 1(a). That is, the feed triangle is identical to the freeze triangle in this case. Other feed velocities compatible with the mass balance are possible, but require adjustment through additional layers to match the otherwise mismatched boundary conditions. For example, in the application, the feed velocity is horizontal, on average, but with mean velocity less than the substrate speed. Our focus here is on the simplest possible illustration. We ignore, among other effects, any boundary layers adjacent to the substrate upstream of the wedge.

The final thickness T of the product is limited by the vertical extent of the flow (not shown in figure 1 but see figure 4). In such a case, solidification is said to be feed-rather than freeze-limited since the heat transfer is not limiting. A Reynolds number based on two-dimensional mean flow rate, TU , is appropriate since the suction of the solidification front draws the fluid, $Re = TU/\nu$. For the application that we consider below, $Re \approx 10^3$, and there can be effectively inviscid flow that is not turbulent, in part because of the stabilizing effect of suction at the solidification front. Such stabilization is familiar from studies of suction on airfoils (e.g. Schlichting 1979).

The flow field of figure 1(a) is inviscid and irrotational. The solidification boundary layer and its mechanism of formation can be understood by considering the introduction of an element of vorticity into that flow. Consider a disturbed flow given by a linear profile (figure 1b),

$$u = U - \omega y. \quad (1.2)$$

The streamlines of figure 1(a) cannot persist since material must now be accelerated to a velocity with components U and $V \cos \theta$ by the time it solidifies. Slower moving fluid must be drawn into regions of faster moving fluid, thereby compressing the linear profile of figure 1(b). The result parallel to the front is shown in figure 2(a). The thickness of the compressed region, δ , can be estimated by equating the shear rate $\omega \sim U/\delta$ from equation (1.2) (recognizing that even though δ is measured normal to the front, for small wedge angles the tangential component of the velocity

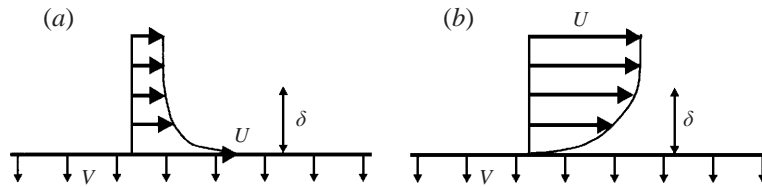


FIGURE 2. Velocity profile (a) for solidification on a moving substrate and (b) for suction applied to flow over a flat plate.

$U \cos \theta \sim U$) to the shear rate due to viscous resistance $\omega \sim \nu/\delta^2$ to obtain,

$$\delta \sim \nu/U. \tag{1.3}$$

Finally, eliminating U in favour of V by the freeze triangle, one finds

$$\delta \sim (\nu/V) \sin \theta. \tag{1.4}$$

This result holds for small but finite wedge angle. This solidification boundary layer, apart from the geometrical factor, scales just like the suction boundary layer (Schlichting 1979; also see figure 2b) if $-V$ is identified with the suction velocity. Material following the streamlines of figure 1(a) is subject to viscous influence over a region of extent δ of figure 1(b). In what follows, we shall restrict attention to infinitesimal wedge angles, $\theta \rightarrow 0$, consistent with the application, where substrate velocity is two orders of magnitude faster than solidification rate, in which case (1.4) reduces to (1.3).

In §2, we revisit the suction boundary layer to understand how advection, diffusion, sources, and sinks contribute to the distribution of vorticity. In §3, we compare and contrast the suction and solidification boundary layers, and in §4, we examine the vorticity budget for planar-flow spin casting where, in addition to a solidification boundary layer, vorticity may be present in the bulk by advection (i.e. other sources). An objective is to understand how bulk vorticity is ‘consumed’ as material solidifies. The physical interpretation of vorticity as twice the angular velocity of a material element holds in both liquid and solid states and at all instants in between.

2. Vorticity flux in a suction boundary layer

It is widely understood, based on theorems of Kelvin and Helmholtz for effectively inviscid flows, that sources and sinks of vorticity can only occur at the boundaries if the flow is incompressible (e.g. Batchelor 1967). Transport occurs by advection and diffusion. The boundary layer on a flat plate (Blasius) provides a classic example. The singularity at the leading edge is the source of vorticity, which simultaneously diffuses away from the boundary and advects downstream. This gives rise to a (viscous) boundary layer of vorticity whose thickness grows with distance as the half-power. The boundary layer develops as the leading-edge vorticity advects downstream and diffuses outward into the irrotational bulk flow.

The Blasius boundary layer analysis is invalid sufficiently close to the leading edge, as is well known. Near the leading edge, the leading-order terms in the solution for the flow are given by Carrier & Lin (1948) (in polar (r, θ) coordinates) as

$$u = Ar^{1/2}(5 \sin \theta/2 + \sin 3\theta/2). \tag{2.1}$$

The flux of vorticity at the wall (1.1), can be shown for this solution to be zero, an

identical result to the similarity solution of Blasius. This result is also consistent with an alternative leading-edge analysis presented by Boley & Friedman (1959). Their stand-off distance for the stagnation point requires a singularity at the leading edge, where all the vorticity in the boundary layer must be generated.

In more general flows, where there is a streamwise bulk pressure gradient, the flux of vorticity at the wall can have either sign depending on the pressure gradient, according to (1.1). Apparently, the boundary can act as either a source or sink of vorticity. After reviewing the established interpretations (Lighthill 1963; Batchelor 1967), Morton (1984) argues, to the contrary, that the wall can only act as a (diffusive) source of vorticity and not a sink. In this view, vorticity decay at the wall may occur only through the generation of *vorticity of opposite sign* which in turn cross-annihilates vorticity adjacent to the wall. We shall illustrate and adopt this interpretation below.

The flux of vorticity in a boundary layer with suction can be analysed using the asymptotic solution first given by Griffith & Meredith (1936), also found in Schlichting (1979). Away from the leading edge, the axial velocity profile is given as (figure 2*b*)

$$u(y) = U_\infty [1 - \exp(v_o y/v)], \quad (2.2)$$

where U_∞ is the (uniform) external velocity and $v = v_o = \text{constant} < 0$ is the vertical velocity. The vorticity is $\omega = (U_\infty v_o/v) \exp(v_o y/v)$, with the maximum value $\omega_o = (U_\infty v_o/v)$ at the wall. Thus, the corresponding flux at the wall is

$$-v(\partial\omega/\partial y)_{y=0} = -U_\infty v_o^2/v < 0. \quad (2.3)$$

This flux is a source of negative vorticity, in the light of Morton's interpretation and the sign of the vorticity. The important difference between the suction boundary layer flow and those analysed by Morton lies in the fact that for suction the wall is a *diffusive source* of vorticity (or upward flux) and simultaneously it is an *advective sink* of vorticity. Indeed, the asymptotic solution for this boundary layer is non-developing since the advective flux of vorticity from the wall, $\omega v_o (> 0)$, is equal in magnitude and opposite in sign to the diffusive flux at the wall $-U_\infty v_o^2/v$. Noting that the bulk pressure gradient is zero for the similarity solution, this can be seen from the boundary condition (e.g. Schlichting 1979),

$$-v \frac{d\omega}{dy} + v_o \omega = \rho^{-1} \frac{dp}{dx}, \quad (2.4)$$

which generalizes the boundary condition (1.1). Therefore, the suction wall produces zero net flux of vorticity, similar to the case of a solid wall without suction. But unlike the Blasius solution, the suction boundary layer (away from the leading edge) does not grow because the viscous diffusion of vorticity away from the wall is matched by an advective flux toward the wall. That is, the diffusive and the advective fluxes are matched for all y , according to the similarity solution (2.2).

The rapid growth of the suction boundary layer, near the leading edge, has been analysed by Iglisch (1949). His solution of Prandtl's boundary layer equations also serves to confirm the simple asymptotic suction solution (Schlichting 1979). A plot of the dimensionless advective and diffusive fluxes against dimensionless downstream distance, $\xi \equiv (-v_o/U_\infty)^2 U_\infty x/v$, is presented in figure 3. As seen in the figure, the match between the advective and diffusive fluxes is valid up to the leading-edge singularity, consistent with (2.4). Thus, as in the case of the no-suction boundary layer, a *net flux of vorticity* into the boundary layer occurs only at the leading-edge singularity. The layer grows until the advective and diffusive fluxes balance for all

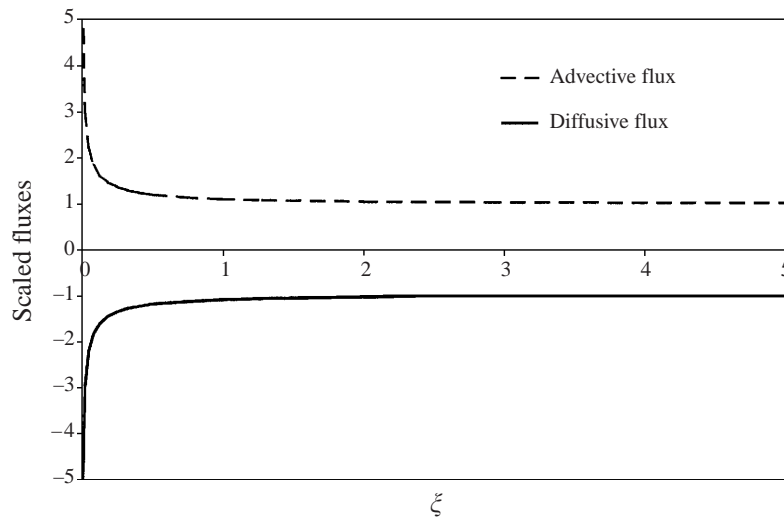


FIGURE 3. Scaled advective (positive) and diffusive (negative) flux calculated from the data of Iglisch (1949) for development near the leading edge of the suction boundary layer.

y. Figure 3 clearly shows that the wall vorticity fluxes reach their asymptotic values relatively quickly (within 10% by $\xi \approx 1$).

3. Suction vs. solidification

In this section, we make the connection between suction and solidification applied to a boundary layer. Figure 2(a) illustrates a solidification boundary layer, and figure 2(b) shows the suction boundary layer. They differ by a translation of the substrate at a velocity U . In practical terms, steady solidification plus uniform translation yields steady suction.

To establish the suction/solidification relationship on a deeper level, one must begin with the full governing equations and boundary conditions appropriate to solidification and examine the boundary layer limit. This has been done for solidification in a narrow gap in the limit corresponding to freezing that is slow relative to substrate translation ($\theta \rightarrow 0$ cf. §1) by Reed & Steen (2001). The main result is that solidification and suction are identical when the appropriate solidification rate (or growth rate of the front) is used as the suction velocity, that is, $v_o = -V$. Through this connection, observations about the effects of suction on boundary layers can be applied to processes that have solidification boundary layers.

4. Application to planar-flow spin casting

In the process called planar-flow spin casting (PFSC; also known as ‘single-roll spin casting’ and ‘planar-flow melt spinning’), molten metal is forced through a die (or nozzle) into the gap between the die and a moving substrate, as illustrated in figure 4. The metal freezes on contact with the substrate wheel (‘single-roll’) and is spun off as a thin strip, sheet or ribbon as described in the patent of Narasimhan (1979). PFSC has been of interest over the past 20 years as a means to produce flat product economically and as a means to rapidly solidify alloys of metallurgical interest. A review from the fluid mechanics point of view is available (Steen & Karcher 1997). For

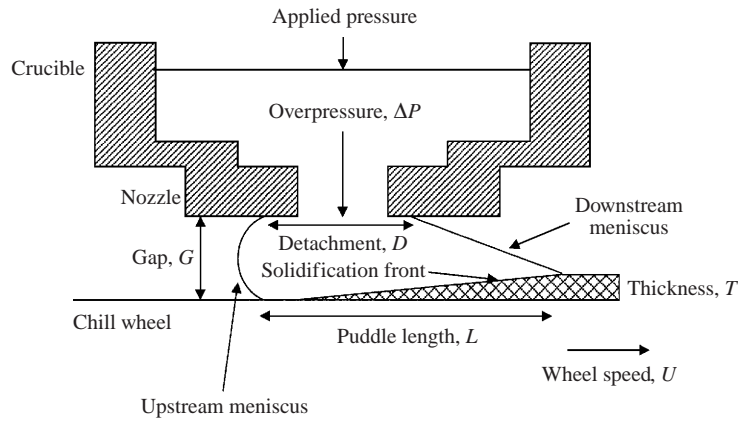


FIGURE 4. Schematic of the liquid puddle and nozzle in planar-flow spin casting (note that horizontal lengths are compressed).

long thin solidification zones, the fluid flow decouples from the heat flow to first order (Carpenter & Steen 1997). A simple justification of this comes from a comparison of conductive to convective thermal transport in their predominant directions (ϕ is temperature),

$$u\phi_x/\alpha\phi_{yy} \sim 0.6.$$

This estimate uses the scales $x \sim L$, $y \sim G$ and $u \sim \bar{u}/2 = (1/2)(T/G)U$ with numerical values given below. The factor 1/2 occurs because mean speed decreases from \bar{u} to zero over the length L . The thermal diffusivity for molten aluminium is $\alpha \sim 0.4 \text{ cm}^2 \text{ s}^{-1}$.

Figure 4 illustrates the region of interest in PFSC. Here the wheel curvature is ignored and the downstream meniscus is idealized as planar, consistent with observation. Vertical lengths are expanded for clarity. Indeed, $L \gg G \gg T$, and $D/L < 1$ since the downstream meniscus is usually gradually sloped. Typically, $L \approx 2 \text{ cm}$, $G \approx 1 \text{ mm}$, $T \approx 0.1 \text{ mm}$ and $D/L \sim 0.1$ with velocities $U \approx 10 \text{ m s}^{-1}$ and $V \approx 5 \text{ cm s}^{-1}$ in experiment. Note that this expansion distorts the slot opening, which is about 3 mm, or about $10^{-1}L$.

Both amorphous and crystalline solids have been cast using the process. In the former case, viscosity varies continuously on cooling whereas, in the latter case, there is a discrete change at the phase-change boundary where latent heat is liberated. We shall assume a sharp solidification front (no 'mushy zone'). For pure metals, morphological instabilities are not possible and the range of cooling rates for which sharp fronts occur make it the typical rather than an exceptional case. Sharp fronts that are nearly linear can be obtained in casting pure aluminium, for example, when the dominant resistance to heat transfer occurs at the product/wheel contact. Thus, the assumptions of paragraph 2 of the Introduction are reasonable for the application.

4.1. Fully developed boundary layer

In PFSC, the boundary layer starts at the upstream meniscus and is limited by the downstream meniscus. 'End' effects are expected both upstream and downstream. The 'entrance' length, due to the developing boundary layer, will be longer than any 'exit' length. Therefore, it is sufficient to verify that the boundary layer development reaches its asymptotic state near the beginning of the puddle region. A Reynolds number (UL/ν) based on the puddle length and wheel speed is $O(10^5)$. The ratio of

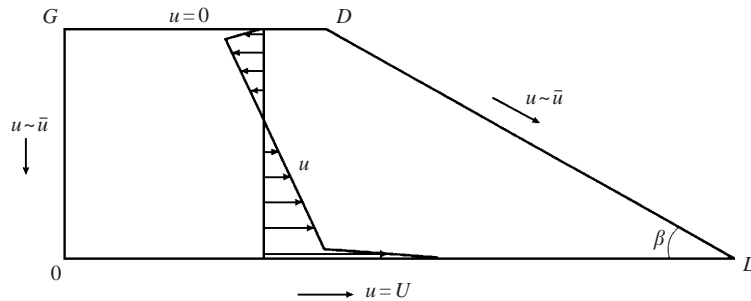


FIGURE 5. Puddle schematic of PFSC for vorticity accounting.

the solidification rate to the wheel speed (V/U) is $O(10^{-2})$. Combining these gives a scaled axial distance $\xi \sim 5$. Since the suction boundary layer reaches 90% of its size for $\xi \sim 1$ (cf. §3), we conclude that the boundary layer is fully developed over most of the puddle region.

4.2. Vorticity distribution

Figure 5 is a simplified rendering of the puddle region, in which the curved upstream meniscus is replaced by a flat section and on which the tangential velocity components are noted. The vertical section $G0$ is just downstream of the nozzle opening. In view of the small nozzle opening, the control volume $OLDG$ actually includes most of the puddle. The velocities on the boundaries are known from the wheel speed, the average fluid velocity (along the free meniscus), and the no-slip condition. A schematic velocity profile suggests a vertical distribution of vorticity. The solidification (bottom) and Blasius (top) boundary layers are inferred based on appropriate Reynolds numbers. The vorticity in the bulk (shown as constant) arises through the history of the establishment of the flow. It can depend on what happens upstream (that is, be advected into the control volume) or what happens during transients before steady conditions prevail. Any vorticity profile must also vary in the horizontal direction, as all the vorticity vanishes as the last material solidifies. Our interest is in confirming the sketch and understanding how the distribution may vary in the horizontal direction.

We estimate the circulation of the flow by two different methods, yielding Γ and Γ_ω , both of which are equivalent by Stokes theorem. The expression for Γ can be simplified to the following, starting from the lower left corner of figure 5:

$$\Gamma \equiv \oint_C \mathbf{V} \cdot d\mathbf{s} = \int_0^L U dx - \int_L^D \bar{u} dx + \int_G^0 \bar{u} dy. \tag{4.1}$$

Here \bar{u} is the average velocity in the bulk, where $\bar{u} \sim UT/G$ by a mass balance between the puddle and the downstream station where all material has been solidified (figure 4). Estimation of the three terms on the right is straightforward:

$$\Gamma \sim UL - (UT/G)(D - L) + (UT/G)G \sim UL, \tag{4.2}$$

since $L \gg G \gg T$ and $D/L < 1$. Not surprisingly, the major contribution to the circulation comes from the bottom solidification boundary.

On the other hand, the vorticity in the flow can be estimated by splitting the region into the solidification boundary layer (*b.l.*) and the bulk,

$$\Gamma_\omega \equiv \iint_A \boldsymbol{\omega} \cdot d\mathbf{A} = \iint_{b.l.} \omega dA + \iint_{bulk} \omega dA. \tag{4.3}$$

In the first term on the right, $\omega \sim U/\delta$ according to (1.2). In the bulk, the vorticity scale is $\partial\bar{u}/\partial y \sim UT/G^2$. The estimate is then straightforward:

$$\Gamma_\omega \sim (U/\delta)(\delta L) + (UT/G^2)(GL) \sim UL. \quad (4.4)$$

Comparing (4.2) and (4.4) shows that both methods lead to the same estimate. The solidification layer contains the dominant contribution to the circulation. We next address how vorticity is removed from the bulk.

The bulk vorticity ω_{bulk} of the velocity profile sketched in figure 5 is constant in the normal direction and much smaller than the solidification layer vorticity. This distribution is consistent with a fully developed uniformly thick layer, as we now show. Indeed, ω_{bulk} can be advected through the layer without disturbing it. This can occur provided the advection of ω_{bulk} is balanced at the boundary by a negative axial pressure gradient, $v_o\omega_{bulk} = \rho^{-1}dp/dx$ (cf. (2.4)). One may think of this pressure gradient as a source of negative vorticity that cross-annihilates the positive vorticity of advection. Provided the balance holds throughout the layer, the solution we have just described is exact, and a straightforward extension of the similarity solution of equation (2.2). In general, the bulk pressure gradient will be ‘imposed’ so that vorticity that shunts across a uniform layer will only be balanced exactly under rather special circumstances. Vorticity can be removed from the bulk in more robust ways and these typically involve a growing or decaying layer, discussed next.

The bulk pressure gradient associated with figure 5 results from a competition between mass removal and area change. Mass removal due to solidification increases pressure while a converging flow under the meniscus (primarily) decreases pressure, according to a Bernoulli balance. Hence, the bulk pressure gradient begins upstream (after the turning region) as positive and weakens downstream to eventually become negative. The change of sign occurs near the meniscus detachment. The streamwise development of the profile can be understood with reference to the position where the bulk pressure gradient vanishes. At that position, in view of the boundary condition (2.4), advection just balances diffusion, consistent with the solidification layer profile sketched in figure 5. Upstream, the adverse pressure gradient acts like a source of positive vorticity and, thus, the solidification layer thins. Downstream, the favourable bulk gradient acts like a source of negative vorticity and the layer thickens. In the top Blasius layer under the nozzle, the negative vorticity is consistent with the adverse bulk gradient. This vorticity cancels the positive vorticity of the bulk, weakening ω_{bulk} in the streamwise direction. Detailed models based on one-dimensional gap-averaged equations are available and relate the pressure gradients to the overall pressure drop; they compare well with experiment (Karcher & Steen 2001; Reed & Steen 2001).

4.3. Under the meniscus

The size of the triangle that characterizes the region under the downstream meniscus is determined by the mass balance to first order. If the flow were irrotational, streamlines would be parallel to the meniscus at an angle β to the front (figure 5), where $\tan\beta = V/U$. The legs of the triangle would be in the same ratio, that is, the triangle would be U/V times longer than high. In reality, the flow has considerable vorticity (cf. figure 2a) and the mean horizontal speed is T/G times slower than U , making the triangle only $(T/G)(U/V)$ longer than high. For experimental conditions, this difference in horizontal extent is a factor of 10 and is easily observable. This is a direct experimental demonstration of the presence of the solidification layer.

We may now postulate a plausible mechanism by which vorticity decreases in the streamwise direction under the meniscus (figure 5). First, near the top boundary, as

the flow passes under the meniscus, the change to a stress-free boundary generates a singular source of opposite sign vorticity (like the leading-edge singularity). This negative vorticity diffuses into the flow, relaxing the velocity profile. Meanwhile, at the bottom boundary, advection of vorticity from the layer weakens in the streamwise direction while under the meniscus the pressure gradient acts as a source of negative vorticity tending to expand the layer and further decrease the net positive vorticity. It should be noted that the curvature of the meniscus implied by the pressure gradient is small and produces negligible vorticity according to estimates based on the analysis of Lugt (1987). While the layer thickens in the streamwise direction, the diffusive and advective fluxes and the pressure gradient decrease as vorticity is removed from the flow. At the downstream end of the meniscus, the solidification layer loses its identity, fluid accelerates to the substrate speed, and essentially no vorticity remains in the flow.

5. Closing remarks

The solidification boundary layer acts like a suction layer, translating at a steady velocity at some wedge angle, opposite in direction to the imposed flow for the suction layer. The thickness scales with the sine of the wedge angle (1.4). A consequence of the change of frame relationship is that solidification layers thin under adverse and thicken under favourable pressure gradients, just the opposite of the case for Blasius layers.

Vorticity is added to or removed from the flow whenever there is an imbalance in the diffusive and (vertical) advective fluxes at the solidification boundary. Addition happens when diffusive flux is larger whereas removal occurs when the advective flux is greater. For solidification layers of positive vorticity, a favourable pressure gradient is required to allow advective removal of vorticity at the solidification front. Removal can also occur through cross-annihilation in the bulk. For PFSC, the bulk pressure gradient in the streamwise direction is adverse under the nozzle where mass removal by solidification dominates and is favourable under the meniscus where the converging cross-section of flow dominates.

This work was partially supported by NSF Grant No. DMI-9712520 and by the Engineering Research Program of the Office of Basic Energy Sciences at the Department of Energy (B. L. R.). A. H. H. would like to thank RPI for granting a sabbatical leave. P. H. S. thanks Alcoa for their continued support of our PFSC work.

REFERENCES

- BATCHELOR, G. K. 1967 *Introduction to Fluid Dynamics*. Cambridge University Press.
- BOLEY, B. A. & FRIEDMAN, M. B. 1959 On the viscous flow around the leading edge of a flat plate. *J. Aero/Space Sci.* **26**, 453–454.
- CARPENTER, J. K. & STEEN, P. H. 1997 Heat transfer and solidification in planar-flow melt-spinning: high wheelspeeds *Int'l J. Heat Mass Transfer* **40**, 1993–2007.
- CARRIER, G. F. & LIN, C. C. 1948 On the nature of the boundary layer near the leading edge of a flat plate. *Q. Appl. Maths* **6**, 63–68.
- GLICKSMAN, M., CORIELL, S. & MCFADDEN, G. 1986 Interaction of flows with the crystal-melt interface. *Ann. Rev. Fluid Mech.* **18**, 307–335.
- GRIFFITH, A. A. & MEREDITH, F. W. 1936 The possible improvement in aircraft performance due to boundary layer suction. *Tech. Rep.* 2315. Rep. Aero. Res. Coun.
- IGLISCH, R. 1949 Exact calculation of laminar boundary layer in longitudinal flow over a flat plate. *Tech. Mem.* 1205. National Advisory committee for Aeronautics.

- KARCHER, C. & STEEN, P. H. 2001 High-Reynolds number flow in a narrow gap driven by solidification i and ii. *Phys. Fluids* (accepted).
- LIGHTHILL, M. J. 1963 Part ii. In *Laminar Boundary Layers* (ed. L. Rosenhead). Oxford University Press.
- LUGT, H. J. 1987 Local flow properties at a viscous free surface. *Phys. Fluids* **30**, 3647–3652.
- MORTON, B. R. 1984 The generation and decay of vorticity. *Geophys. Astrophys. Fluid Dyn.* **28**, 277–308.
- NARASIMHAN, M. C. 1979 US Patent **4** 142 571.
- REED, B. L. & STEEN, P. H. 2001 Inviscid flow in a long, thin gap with solidification. *J. Fluid Mech.* (to be submitted).
- SCHLICHTING, H. 1979 *Boundary-layer Theory*, 7th edn. McGraw-Hill.
- STEEN, P. H. & KARCHER, C. 1997 Fluid mechanics of spin casting. *Ann. Rev. Fluid Mech.* **29**, 373–397.